1993

Transient Laser Cooling

S. Padua
State University of New York, Stony Brook, New York

C. Xie
State University of New York, Stony Brook, New York

R. Gupta
State University of New York, Stony Brook, New York

Herman Batelaan
University of Nebraska-Lincoln, hbatelaan@unl.edu

T. Bergeman
State University of New York, Stony Brook, New York

See next page for additional authors

Transient Laser Cooling

S. Padua, C. Xie, R. Gupta, H. Batelaan, T. Bergeman, and H. Metcalf
Physics Department, State University of New York, Stony Brook, New York 11790
(Received 17 February 1993)

We observed a new type of sub-Doppler cooling that employs neither polarization gradients nor magnetic fields, and involves neither a damping force nor significant diffusive heating. Instead, light shifts combined with optical pumping (OP) to levels not coupled by the laser field gives transient cooling, and steady state is not achieved. The time scale is set by the OP rate. We observe both cooling and heating, but often with the opposite detuning from that of steady state. A semiclassical and a fully quantum mechanical calculation of transient cooling agree very well with one another and with our data.

PACS numbers: 32.80.Pj

Laser cooling of neutral atoms requires velocity-dependent optical forces that arise from the motion of an atom in a nearly resonant light field. If the selection rules require that excited atoms spontaneously decay to only the initial state, the velocity-dependent interaction arises from the Doppler shift of the laser-driven transition. In this case one readily calculates a minimum achievable temperature called the Doppler limit, $T_D = \hbar\gamma/2k_B$, where $\tau \equiv 1/\gamma$ is the excited-state lifetime [1]. By contrast, if the ground state has multiple sublevels accessible from the excited state, much lower temperatures are achievable [2–4]. The transitions from these sublevels may be driven by different polarizations, and thus sub-Doppler temperatures are often associated with polarization gradients. The cooling force derives from the failure of the internal state of moving atoms to follow adiabatically the changing optical environment of a spatially inhomogeneous optical field, such as that produced by light beams of different polarizations.

For slow enough atomic velocities, however, this nonadiabatic part of the force is small compared with the velocity-independent force that derives from the spatially varying light shifts of the atoms. In a standing wave, this conservative force produces channels that can strongly influence atomic motion or even confine atoms in $\lambda/2$ size regions [5,6]. Furthermore, spontaneous decay in a standing wave can provide the irreversible process needed to produce a dissipative force that cools atoms [7].

We report here a theoretical and experimental study of sub-Doppler atom cooling achieved by transient effects of laser excitation. We have found that cooling and heating can occur when the atom goes through only a few optical pumping (OP) cycles, but often with opposite detuning from that of steady-state situations. In most other types of sub-Doppler laser cooling, a damping force $\mathbf{F} = -\mathrm{tr}(\rho\nabla\mathcal{H})$ can be computed from the steady-state solution of the optical Bloch equations for the density matrix ρ. This is appropriate because the laser cooling processes generally continue for times long compared with OP transients. In transient laser cooling, the time scale is set by the OP rate to a ground state that is not coupled to an excited state by the laser field ("dark state") so steady-state solutions are inappropriate and a damping force cannot be defined [8].

For an intuitive understanding of how transient cooling works, consider the conservative motion of atoms that enter a standing-wave field nearly transverse to its $\mathbf{k}$ vectors, but with a small velocity component v_z of a few cm/s parallel to $\mathbf{k} = k\hat{\mathbf{z}}$. Such atoms experience a spatially varying light shift potential $U(z) = U_0 \sin^2(kz)$ that produces a sinusoidal force. (U_0 takes the sign of the detuning $\delta \equiv \omega_{\text{laser}} - \omega_{\text{atom}}$ and is proportional to the intensity at low intensity.)

The atoms experience this force until they are optically pumped to a dark state. Since the OP rate $\gamma_p(z) \equiv \tilde{\gamma}_p \times \sin^2(kz)$ vanishes at the nodes, OP is slower for atoms that enter the standing wave near a node, and thus the average kinetic energy (KE) change is greater for such atoms. For $\delta > 0$, more KE is lost by atoms moving away from a node than gained by atoms moving away from an antinode, so on average atoms lose KE [Fig. 1(a)] and conversely for $\delta < 0$ [Fig. 1(b)]. This contrasts with other types of cooling where the optical force may either heat or cool the atoms depending on both the angular momentum scheme ($F_g - F_e$) and the detuning: Here $\delta > 0$ always gives cooling.

We have performed classical trajectory calculations based on the above model by integrating the equation $m\ddot{z} = kU_0 \sin(2kz)$. For initial conditions we choose v_0 and z_0 distributed uniformly in the intervals $[-30, 30]$ cm/s and $[0, \lambda/2]$, respectively. In the weak excitation approximation, the upper state can be neglected, and the ground-state potential amplitude $U_0 = 2\hbar s C\delta/L$, where $s = I/I_{\text{sat}}$ is the laser saturation parameter, C is the strength of a particular transition, and $L = 1 + (2\delta/\gamma)^2$. The saturation intensity for the strongest component of this transition ($C = 1$) is $I_{\text{sat}} = hc/\lambda^3\tau \cong 1.6$ mW/cm^2 in Rb, where $\tau = 1/\gamma \cong 27$ ns.

From the solution $z(t)$ to these equations of motion we find the OP rate $\gamma_p(t) = \tilde{\gamma}_p \sin^2[kz(t)]$, where $\tilde{\gamma}_p = 2sC \times B\gamma/(L + sC)$ and B is the branching ratio to the dark states. Then the probability of OP between t and $t + dt$ is $P(t)dt = \gamma_p(t) \exp[-\int_0^t \gamma_p(t')dt']dt$. The primitive of $P(t)$ is then inverted to find a distribution of pumping times. A Monte Carlo approach uses these pumping times to terminate the classical motion, and the resulting

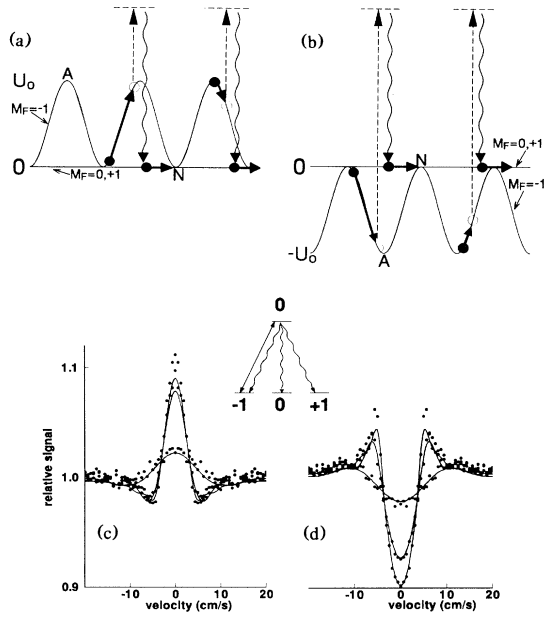

FIG. 1. (a) The light shift potential and optical pumping scheme for $\delta > 0$. Atoms entering near a node travel further before OP, and therefore lose more KE than atoms entering near an antinode, which travel a shorter distance before OP. (b) Similar to (a), but for $\delta < 0$ atoms gain more KE than they lose. (c) Velocity distributions found from the semiclassical calculation (dots) for the transition shown in the inset. Here $s = 0.66$ and $\delta = +12$ MHz (as in Fig. 3). "Snapshots" of the velocity distribution are made at times 3, 6, and 9 μs. The solid lines show the results of quantum mechanical calculations for the same conditions. (d) Similar to (c) but for $\delta = -12$ MHz. Inset: One of the simplest level schemes for transient cooling, $F_g = 1 \rightarrow F_e = 0$ with σ^+ excitation.

velocity distribution is calculated.

We have applied this approach to the simplest atomic scheme of the classical scheme above, an $F = 1 \rightarrow 0$ transition with σ^+ excitation, shown in Fig. 1 (inset). Results of these calculations are shown in Figs. 1(c) and 1(d) (dots). The sharp features in Fig. 1(d) for $\delta < 0$ occur at stationary points where $E_{\text{kin}} = U_0$. It is clear that this simple model of transient laser interactions gives cooling for blue detuning and heating for red detuning for this $F = 1 \rightarrow 0$ transition.

Figures 1(c) and 1(d) also show remarkable agreement between the classical results and results of a fully quantum mechanical calculation including the excited state explicitly (solid lines). The sharp cooling and heating features in the classical results are smoothed in the quantum results. We attribute this to neglect of the uncertainty in position and of recoil in the classical calculation.

We can estimate the velocity capture range of transient blue cooling for atoms that move freely without being channeled between the planes of the standing waves. The probability of OP in time t_1 is $P(t_1) = \int_0^{t_1} \gamma_p(z) dt$ for $P(t_1) \ll 1$. To find the mean distance z_1 from a node where OP occurs, we use $dt = dz/v_z$ and set

$$\int_0^{z_1} [\gamma_p(z)/v_z] dz = \int_{z_1}^{\pi/2k} [\gamma_p(z)/V_z] dz .$$

For $E > 2U_0$, the variation of v_z with z has little effect on z_1 so it comes out of the integrals, and we find $\sin^2(kz_1) = 0.83$. Thus atoms undergo OP from a position where their average light shift (potential energy) is $\sim \frac{5}{6} U_0$, and since their initial spatial distribution was uniform so their average initial potential energy was $U_0/2$, the average total energy change is $\Delta E \sim -U_0/3$. This is a mechanical energy loss for $U_0 > 0$ ($\delta > 0$) and a gain for $U_0 < 0 (\delta < 0)$. This process does not make a very large change in the velocity distribution for atoms with E more than a few times U_0 because $\Delta v_z/v_z = \Delta E/2E \sim -U_0/6E$. This estimate of the capture velocity is consistent with the detailed computational results of Fig. 1 and with the data.

In this transient cooling process, the final velocity distribution does not result from competition between a steady-state damping force and diffusive heating. Instead we find the changes in KE are bounded by U_0. The widths of the cooling peaks (and heating dips) in the measured velocity distributions decrease with intensity so that widths substantially below the Doppler limit are attainable, as shown by our measurements.

The experiments use a thermal beam of natural Rb produced by an oven at $T \sim 150\,^\circ$C with horizontal slit aperture 0.06 mm high by 2 mm wide, and a vertical beam defining slit 2 mm high by 0.06 mm wide about 35 cm away [9]. The atoms emerge from the vertical slit in a fan-shaped beam and then interact with a pair of counterpropagating laser beams transverse to the atomic beam axis. The nearly flat atomic beam profile is measured with a scanning hot platinum-tungsten wire, 25 μm in diameter, 1.3 m away from the region of interaction with the laser beam. Three square Helmholtz coil pairs cancel the Earth's field.

A 35 mW Sharp LT025 diode laser is locked at the $5S \rightarrow 5P$ transition of Rb near $\lambda = 780$ nm by saturated absorption in a vapor cell at room temperature. The spatial intensity profile of the 23 mm long $\times 5$ mm high laser beam is flattened to a few percent by a tilted etalon [10]. For thermal velocity atoms ($\bar{v} \sim 350$ m/s) the average interaction time is 63 μs. The turn-on and turn-off edges of the light field are sharpened by an aperture and diffraction limited to about 0.3 mm, corresponding to an entrance and exit time of < 1 μs for atoms at thermal velocity. For most experimental conditions, the OP time is longer than 1 μs.

In order to explore the phenomena sketched above, we have measured the transverse velocity distribution of our atomic beam after it passes through the circularly polarized standing wave in zero magnetic field. For the $F_g = 1 \rightarrow F_e = 2$ transition of ^{87}Rb (dashed line in Fig. 2), OP to the dark state $F_g = 2$ is allowed. Figure 3(a) shows clear evidence of cooling for light detuned blue by

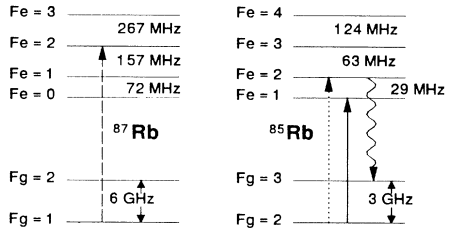

FIG. 2. The hyperfine energy level scheme of the Rb isotopes showing transitions of interest in this paper.

$\delta = +12$ MHz ($\cong 2\gamma$) from this transition, and Fig. 3(b) shows heating for $\delta = -12$ MHz. This demonstration of blue cooling (sub-Doppler) and red heating appears in all our data for all the allowed transitions of Fig. 2.

Figure 3(a) shows significant blue cooling even with s lowered to ~ 0.066 by a neutral density (ND = 2) filter. At this intensity, the average OP time $\bar{\tau}_p \equiv 1/\bar{\gamma}_p$, found by averaging γ_p over a wavelength and over the various transitions, is 64 μs. (Typically, $\tilde{\gamma}_p/\bar{\gamma}_p$ ranges from 2 to 4.) This is fortuitously close to the average 63 μs interaction time for atoms in our thermal beam. When the interaction region is shortened from the 23 mm of Fig. 3(a) to only 1.4 mm, corresponding to an average interaction time of only 4 μs, there is still clear evidence of cooling on the blue side for $s \cong 6.6$.

Excitation of ^{85}Rb on the $F_g = 2 \rightarrow F_e = 1$ transition (solid line of Fig. 2) presents a close analog to the $F_g = 1 \rightarrow F_e = 0$ model discussed above, because the $F_e = 1$ state cannot decay to $F_g = 3$. However, OP can occur to the $F_g = 2$, $M_F = +1$ and $+2$ magnetic sublevels, which are "dark" in our σ^+ light. The low intensity data near the top of Fig. 4(a) clearly show cooling signals with σ^+ light detuned $+6$ MHz blue of this $F_g = 2 \rightarrow F_e = 1$ transition. At the lowest intensity of Fig. 4(a) (top trace), U_0/h is only 11 kHz so the expected change in the velocity of an atom is less than the recoil velocity $\hbar k/M$, the transient cooling effects are washed out by the momentum changes from the random direction of spontaneous emission.

At higher intensity, a second phenomenon appears. Light tuned 6 MHz blue of this $F_g = 2 \rightarrow F_e = 1$ transition of ^{85}Rb is also 23 MHz red of the $F_g = 2 \rightarrow F_e = 2$ transition (dotted line of Fig. 2). Although atoms optically pumped to the $(F_g, M_F) = (2,1)$ sublevel cannot be excited to $F_e = 1$ with σ^+ light, there is an allowed transition to the $(F_e, M_F) = (2,2)$ sublevel. Since this state can decay to the $F_g = 3$ dark state (wiggly line in Fig. 2), transient effects can occur. Using $\bar{\tau}_p$ calculated as before, we find the rate for this further off-resonant transition to be significant only at high enough intensity. This slower process involves light tuned red of resonance, so it heats instead of cools the atoms as shown in the high intensity traces of Fig. 4(a). The data of Fig. 4(a) clearly show a change from cooling to heating as s increases

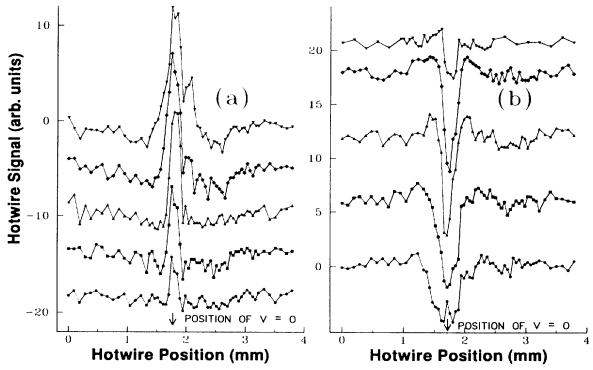

FIG. 3. (a) Measured atomic beam profiles for circularly polarized light tuned 12 MHz blue of the $F_g = 1 \rightarrow F_e = 2$ transition of ^{87}Rb. The intensities are 0.1, 0.3, 1.0, 3.0, and 10 mW/cm^2 (bottom to top), and the saturation intensities for the three magnetic components are 19.2, 6.4, and 3.2 mW/cm^2 (3.2 for $M_F = 1 \rightarrow 2$). The vertical scale's arbitrary units are $\sim 1\%$ of the atomic beam intensity. For the mean longitudinal velocity of 350 m/s, a 37 μm displacement represents 1 cm/s, so the width of the third peak (saturation $\cong 1$ for $M = 1 \rightarrow 2$) is 6 cm/s, corresponding to about $\frac{1}{2}$ of the Doppler limit. (b) Similar results for light tuned 12 MHz red of the same transition.

from 0.3 to 1.0 for our 63 μs interaction time, corresponding to $\bar{\tau}_p$ going from 80 to 24 μs.

We can also observe this phenomenon by varying the interaction time at fixed s. Figure 4(b) shows transient cooling on this $F_g = 2 \rightarrow F_e = 1$ transition at short times,

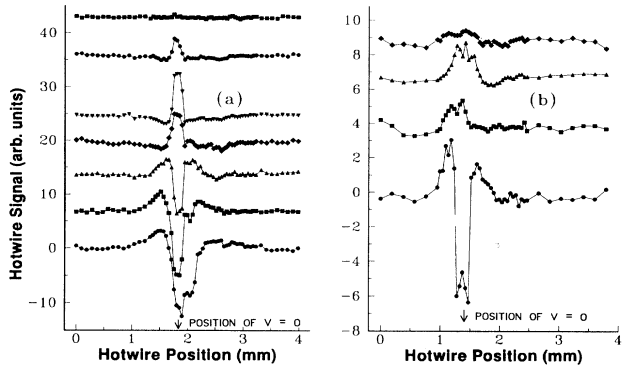

FIG. 4. (a) Measured atomic beam profiles for circularly polarized light tuned 6 MHz blue of the $F_g = 2 \rightarrow F_e = 1$ transition of ^{85}Rb. The intensities are 10, 3.0, 1.0, 0.3, 0.16, 0.03, and 0.01 mW/cm^2 (bottom to top), and the saturation intensities for the three components are 16, 5.3, and 2.7 mW/cm^2 (16 for $M_F = 0 \rightarrow 1$). For the mean longitudinal velocity of 350 m/s, a 37 μm displacement represents 1 cm/s, so the width of the fourth peak is 4 cm/s, corresponding to about $\frac{1}{3}$ of the Doppler limit. (b) Similar data for interaction times of 32, 16, 8, and 4 μs (bottom to top). Cooling becomes heating at higher intensity or longer interaction time.

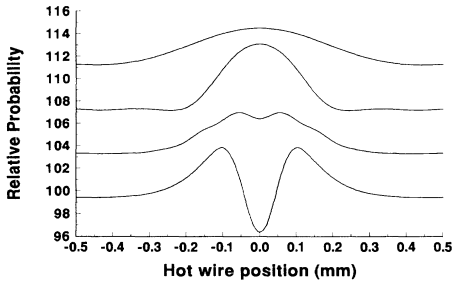

FIG. 5. Velocity distributions found from the fully quantum calculation with $F_g=2$, $F_g=3$, $F_e=1$, and $F_e=2$ internal states included, using appropriate excitation and decay matrix elements. The saturation parameter is taken to be 0.4 and the detuning is 6 MHz above the $F_e=1$ state, as for the experimental data in Fig. 4(b). The successive curves correspond to interaction times of 4, 8, 16, and 32 μs for the most probable longitudinal velocity in the beam.

but heating as the interaction time increases from 16 to 32 μs at $s=0.35$. In this case atoms in $(F_g,M_F)=(2,1)$ are given enough time for excitation to $F_e=2$. There is also a small but persistent and repeatable upward peak from the bottom of the heating dip in the high intensity data of Fig. 4(a) and in the long time data of Fig. 4(b). It may come from the $(F_g,M_F)=(2,2)$ atoms that are not heated by excitation to $F_e=2$. All the features of Fig. 4 have also been observed on the $F_g=1\rightarrow F_e=0$ transition of ^{87}Rb.

As a further illustration of this transient cooling model, we have added a small magnetic field transverse to the axis defined by the circularly polarized standing wave ($\mathbf{B}\perp\mathbf{k}$). When the Larmor frequency is large enough to precess atoms in the $(F_g,M_F)=(2,1)$ or (2,2) dark states back to the coupled (2,0) state faster than they can be optically pumped to the $F_g=3$ dark state (via $F_e=2$, wiggly line in Fig. 2), the cooling persists to the higher intensities shown in Fig. 3(a).

Multistate processes are difficult to model accurately with classical trajectory calculations, but we have developed a fully quantum mechanical model [11]. The change from cooling to heating shown in Fig. 4 provides an opportunity for sensitive tests of such quantum mechanical calculations. The basis set consists of product states of internal and external atomic coordinates [12]. The set of internal states includes typically two ground and two excited levels so the calculation is not restricted to low excitation rates. The external, center-of-mass motion states are free particle wave functions, allowing inclusion of the recoil effect in every optical transition. The density matrix calculated in this basis includes optical coherence (off-diagonal elements) to sufficiently high order so that the calculated velocity distribution converges. Equations for the temporal evolution of the density matrix are obtained from the optical Bloch equations.

Figure 5 shows the results from these quantum calculations for parameters corresponding to Fig. 4(b). The experimental conditions, including the longitudinal velocity distribution and instrumental resolution, have been carefully modeled. The transverse velocity distribution flips from cooling to heating as in the experiments, but there is an unexplained discrepancy of about a factor of 2 in the width of the final heating dip.

There are various repumping methods that might allow recycling of atoms for further cooling by this technique [7]. Furthermore, it can readily be extended to 2D or maybe even 3D. Also, this technique might be applied to atoms with a first transition in the deep ultraviolet and a metastable state where traditional cooling techniques are difficult to implement. For example, atomic hydrogen in its $2S$ state could be cooled this way on the easily produced Balmer-α line at 656 nm. Similar possibilities exist in singlet He, rare gases, and alkaline earth D states.

In summary, our experiments with a Rb atomic beam and a transverse standing-wave laser field have demonstrated a new mechanism for sub-Doppler laser cooling. This mechanism requires no polarization gradients or magnetic fields. It operates on a short time scale, determined by the OP times. We have developed a theoretical model with classical trajectories and have also applied a fully quantum mechanical treatment. These models give results close to each other and to the measurements.

This work was supported by NSF, ONR, AFOSR, and CAPES (Brazil). The quantum calculations were performed at the Cornell National Supercomputer Facility, funded by NSF and IBM.

[1] D. Wineland and W. Itano, Phys. Rev. A **20**, 1521–1540 (1979).
[2] P. Lett *et al.*, Phys. Rev. Lett. **61**, 169 (1988).
[3] J. Opt. Soc. Am. **5**, 1961–2288 (1989) (special issue).
[4] B. Sheehy *et al.*, Phys. Rev. Lett. **64**, 858 (1990).
[5] C. Saloman *et al.*, Phys. Rev. Lett. **59**, 1659 (1987).
[6] C. Westbrook *et al.*, Phys. Rev. Lett. **65**, 33 (1990).
[7] A. Aspect *et al.*, Phys. Rev. Lett. **57**, 1688 (1986).
[8] O. Emile, R. Kaiser, C. Gerz, H. Wallis, A. Aspect, and C. Cohen-Tannoudji (to be published).
[9] S.-Q. Shang *et al.*, Phys. Rev. Lett. **65**, 317 (1990); S.-Q. Shang *et al.*, in *Atomic Physics 12*, edited by J. Zorn and R. Lewis (World Scientific, Singapore, 1991), p. 105.
[10] C. Xie *et al.*, Opt. Lett. **18**, 173 (1993).
[11] T. H. Bergeman (to be published).
[12] Y. Castin *et al.*, in *Light Induced Kinetic Effects on Atoms*, edited by L. Moi *et al.* (ETS Editrice, Pisa, Italy, 1991).